The structure and ferroelectric property of La-doped BiFeO$_3$/SrTiO$_3$ artificial superlattice structure by rf sputtering: Effect of deposition temperature

Shang-Jui Chiu [a,b], Yen-Ting Liu [c], Ge-Ping Yu [a,d,*], Hsin-Yi Lee [b], Jia-Hong Huang [a]

[a] *Department of Engineering and System Science, National Tsing Hua University, Hsinchu 30013, Taiwan*
[b] *National Synchrotron Radiation Research Center, 101 Hsin-Ann Road, Hsinchu Science Park, Hsinchu 30076, Taiwan*
[c] *Program for Science and Technology of Accelerator Light Source, National Chiao Tung University, Hsinchu 300, Taiwan*
[d] *Institute of Nuclear Engineering and Science, National Tsing Hua University, Hsinchu 30013, Taiwan*

ARTICLE INFO

ABSTRACT

Improvement of ferroelectric property by Lanthanum (La)-doping of BiFeO$_3$ (BFO) and strain effect of high quality superlattice films deposited at temperature $\geqq 700$ °C was shown in this study. The in-pane (200) radial scans showed that films at deposition temperature above 700 °C behaved high strained ~−1.4% and showed epitaxity properties. The La-doped BFO superlattice structure also behaved higher polarization value ~197 μC/cm^2 and lower leakage current density comparing with BFO superlattice structure shown in our previous study. The ferroelectric properties of superlattice structures are enhanced by lattice strain and strongly correlated with the defect state of films.

© 2012 Elsevier B.V. All rights reserved.

1. Introduction

Bismuth iron oxide (BFO) is a popular lead-free ferroelectric material with high remnant polarization which has attracted much attention for fundamental studies and technological applications, for instance, dynamic random access memory and nonvolatile memory [1,2]. In spite of the great properties of BFO, a serious problem with BFO including high leakage current and ferroelectric reliability resulted from oxygen stoichiometry, Bi vacancy and Fe^{2+} cation [3,4], which resulting in increasing of the concentration of free carriers and degradation of ferroelectric properties, is a challenge for the application of BFO.

To overcome the problem of BFO materials, several methods were studied in previous research. The epitaxial artificial superlattice structure is one of the methods to enhance properties by controlling the c over a value with relativity mismatch of lattice constant between two or more kinds of materials and solve the problems of Perovskite materials. Previous researches [5–7] have shown that BTO and SrTiO$_3$ (STO) artificial superlattice have better ferroelectric and dielectric properties than single layer BTO, STO films. Symmetric BFO and STO superlattice have also been prepared to investigate the relationship between superlattice formation and ferroelectric properties in the early work [8–10]. In our previous study, the enhancement of deposition temperature and strain state on asymmetry BFO/STO superlattice structure also has been investigated [11]. Besides, recent study has also focused on substitution of element [12–19] and solid solutions [20,21] to enhance the

ferroelectric properties of perovskite materials. It has been reported that substitution of Bi^{3+} by La^{3+} with similar radii with Bi^{3+} could reduce Bi volatilization and vacancy concentration of oxygen in BFO [22–24].

Although one may find the researches about effective strain effect and substitution effect on the structure and ferroelectric properties of BFO thin films, the information about combination of those effects is still not well understood. A further study of the integration of substitution effect and strain enhancement effect on BFO material with La^{3+} doping is carried in this study. The objective of this work is to research the role of La^{3+} doping on the ferroelectric properties of La-doped BFO/STO superlattice films deposited by sputtering system. By controlling deposition temperature, the relationship between strain, crystal structure and ferroelectric properties of La-doped BFO/STO superlattice will also be discussed.

2. Experimental details

The asymmetric (t$_{La-BFO}$/t$_{STO}$ = 4.0 nm/1.0 nm) 5% La-doped BFO/STO superlattice films were prepared by triple-gun rf-magnetron sputtering system on conductive Nb-doped STO (001) substrates with La-doped BFO and STO in sequence 10 layers. The superlattice structures were deposited at various substrate temperatures ranging from 600 °C to 850 °C. The detail of the experimental was described in our previous study [11].

X-ray reflectivity measurements were performed using CuKα$_1$ radiation in a standard Huber two-circle X-ray diffractometer (operated at 50 kV and 200 mA). Bede Mercury code [25] was used to the fit reflectivity data to determine the roughness, thickness and density of the superlattice structure. The high-resolution diffraction patterns

---

were measured using a synchrotron X-rays source at wiggler beamline BL-17B1 in the National Synchrotron Radiation Research Center (NSRRC), Hsinchu, Taiwan. The typical scattering vector resolution in the vertical scattering plane was set to ~1×10^{-3} nm^{-1} in these experiments.

An atomic-force microscope (AFM) was used to examine the surface morphology of the films. The AFM image was recorded on an instrument (Digital Instrument MultiMode AFM) operated in contact mode with silicon tip (diameter <20 nm). Various areas (2×2 μm^2) of the surfaces were scanned at a scan rate of 0.8 Hz, and the root-mean-square surface roughness A was automatically calculated by a computer program. For measurements of electrical properties, Pt top electrodes were sputtered onto the surface of the superlattice films near 25 °C. The ferroelectric hysteresis loop at frequency 1 kHz and 25 °C and leakage current measurements of La-doped BFO/STO superlattice films at various temperatures were measured with aix-ACCT TF-2000 analyzer.

3. Results and discussion

Fig. 1 plots the reflectivity curves and the best fitting results of La-doped BFO$_{4nm}$/STO$_{1nm}$ superlattice films with various deposition temperatures. The typical shape of the reflectivity curves and the clear oscillations therein demonstrate that both the surface and the interface are smooth and are near coherent. The appearance of Bragg peaks and Kisseig fringes with equal space confirms vertical periodicity of superlattice films. The results of fitting the reflectivity curves, presented in Table 1, reveal that the density of the La-doped BFO and STO sublayers increases at deposition temperature ranging from 650 °C to 750 °C. For all superlattice structures, the films that were deposited at 750 °C had the highest density—very close to the perfect value for bulk BFO/STO materials, which reveals much lower concentration of defect than other samples. The La-doped BFO/STO superlattice structure has a stable thickness, indicating that the deposition temperature does not affect the rate of growth. The fitted results also demonstrate that the surface and interface roughness increased with deposition temperature. Table 1 presents the surface roughness of the superlattice structure observed by AFM. The root-mean square surface roughness exhibits a trend similar to that of the fitted reflectivity curves, which increase with deposition temperature.

Fig. 2 shows (0 0L) radial scan of superlattice films with an STO lattice parameter of 0.3905 nm at 25 °C, for various deposition temperatures. At a deposition temperature ≧700 °C, the diffraction pattern of superlattice films exhibit a main line and satellite lines with

Table 1
Parameters obtained from best-fit results of reflectivity curves of La-doped BFO/STO superlattice films deposited on an Nb-doped STO substrate at different deposition temperatures. The surface roughness determined from AFM measurements is listed in the last column for comparison. The relative standard deviations of the fitted data are for thickness below 2%, density below 2% and roughness below 6%. The thickness of the SrTiO$_3$ substrate is set as infinite and the bulk density is 5.118 g/cm^3. The bulk density of La-doped BFO is 8.354 g/cm^3 and that of STO is 5.118 g/cm^3.

Deposition temperature (°C)	Fitted thickness (nm)		Fitted density (g/cm^3)		Fitted roughness (nm)			AFM (nm)
	T_{BFO}	T_{STO}	P_{BFO}	P_{STO}	$\sigma_{BFO/sub}$	$\sigma_{interface}$	$\sigma_{surface}$	$\sigma_{surface}$
600	4.12	0.99	7.60	4.66	0.4	0.7	0.53	0.52
650	3.91	0.92	7.85	4.86	0.41	0.69	0.56	0.41
700	3.97	0.91	7.94	4.91	0.42	0.7	0.59	0.67
750	3.97	0.91	8.02	5.02	0.42	0.7	0.59	1.47
800	3.9	0.94	7.52	4.81	0.45	0.9	0.65	2.14
850	4.01	0.92	7.52	4.61	4.5	0.92	0.92	2.77

clearly discernible Pendellösung fringes, indicating the superior crystalline quality and interface quality of the La-doped BFO/STO superlattice structure. Moreover, the satellite peaks with equal space also prove periodicity of superlattice films. When the deposition temperature was increased to 800 °C, the position of the main diffraction line of the superlattice does not change but the period of the satellite lines changed. Increases in interface roughness, surface roughness and inter-diffusion with temperature may have been responsible for these changes of period.

Fig. 3 displays the crystal truncation-rod spectra of the superlattice films in the direction [H 0 0]. Superlattice films that were deposited at a temperature over 700 °C yield a diffraction peak which overlaps with peaks of the STO substrate, revealing that the La-doped BFO/STO superlattice is well-strained by the STO substrate; relaxation of strain is almost entirely not observed. The in-plane strain of the samples is also shown in the right side of Fig. 3. The horizontal lattice parameter is given by the equation $a = H\lambda/2\sin\theta$, where H denotes the location of the Bragg diffraction expressed in reciprocal lattice units (r.l.u), and θ denotes the measured Bragg angle. All of the superlattice films have a horizontal lattice parameter smaller than the lattice constant of bulk BFO (0.396 nm), which finding is strong evidence of the compression of the BFO lattice by the STO substrate. The in-plane strain of a superlattice film (ε_{xx}) is given by the equation, $\varepsilon_{xx} = (a_x - a_{x0})/a_{x0}$, where a_x is the lattice parameter of the strained layer, and a_{x0} is the lattice parameter of strain-free layer. The superlattice films that are deposited at
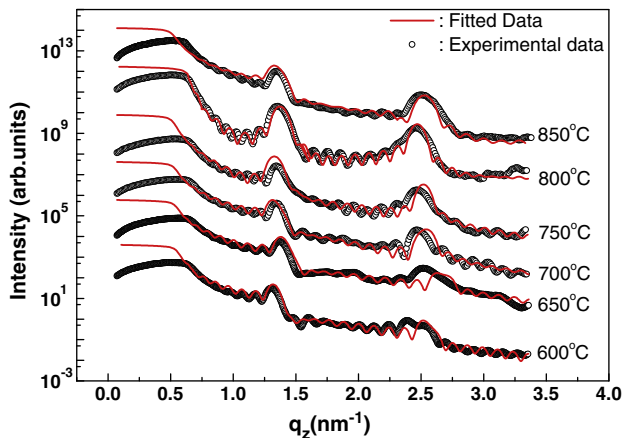

Fig. 1. Measured reflectivity curves (circles) of La-doped BFO/STO superlattice films deposited at substrate temperatures between 600 °C to 850 °C with the best curve fitted results (solid line).
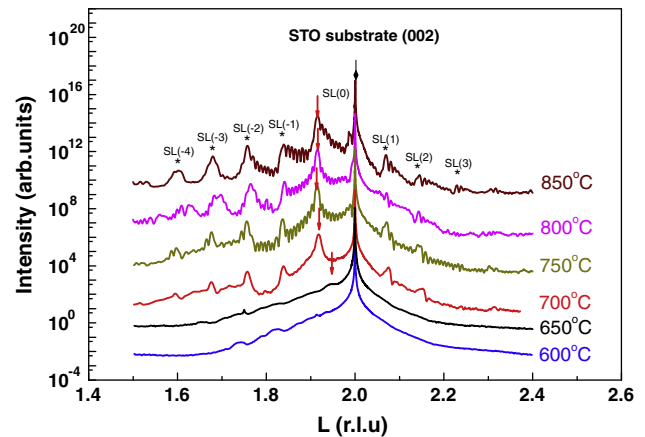

Fig. 2. Intensity distribution of a (002) radial scan of La-doped BFO/STO superlattice films deposited at substrate temperatures between 600 °C to 850 °C. These results reflect high quality layer-by-layer superlattice structure. An arrow marks the position of the superlattice main peak and a dashed line denotes the position of the mean value of the superlattice.
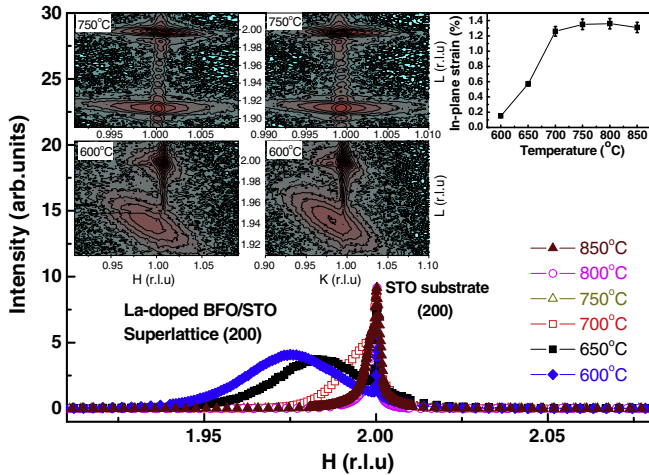
Fig. 3. X-ray intensity of radial scans along the (200) in-plane Bragg peak of La-doped BFO/STO superlattice films deposited at different substrate temperatures. The right side shows an in-plane compressive strain of BFO layer as a function of deposition temperature, and the reciprocal space maps of the samples are also shown in the left side of Fig. 3.

a temperature of over 700 °C have a higher in-plane strain which approaches the critical value of 1.42% associated with a fully strained BFO sublayer than those deposited at 600 °C or 650 °C. The in-plane strain of films does not change as the deposition temperature increases above 700 °C. The reciprocal space maps of the samples are also shown in the left side of Fig. 3. The profile indicates that La-doped BFO/STO superlattice deposited at 750 °C exhibits profile with similar H and K index of films and substrate, which indicate that the superlattice films are isometrically strained by STO substrates. The symmetry profile with uniform L index of superlattice films reveals that superlattice behave well strain effect. However, the higher L index and non-symmetry diffraction profile of superlattice films deposited at 600 °C demonstrate the larger partial strain relaxation of superlattice films.

Fig. 4 shows the full width at half-maximum of the in-plane rocking curves of La-doped BFO/STO superlattice films, which decrease rapidly as the deposition temperature increases. Superlattice films that are prepared at a temperature of over 700 °C exhibit have a better crystalline quality than others. The slight broadening of the diffraction peak demonstrates the reduction in the crystalline quality of the superlattice films as the deposition temperature increases above 800 °C.

Fig. 5(A) presents the hysteresis loops of La-doped BFO/STO superlattice films. At a deposition temperature of $\leqq$750 °C, La-doped BFO/STO films have excellent crystalline quality and clear
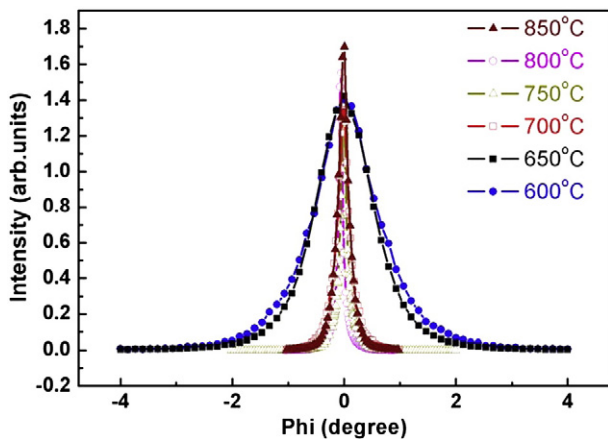

Fig. 4. FWHM of in-plane rocking curves of La-doped BFO/STO superlattice structure. The best crystal quality is displayed with superlattice films deposited at 750 °C.
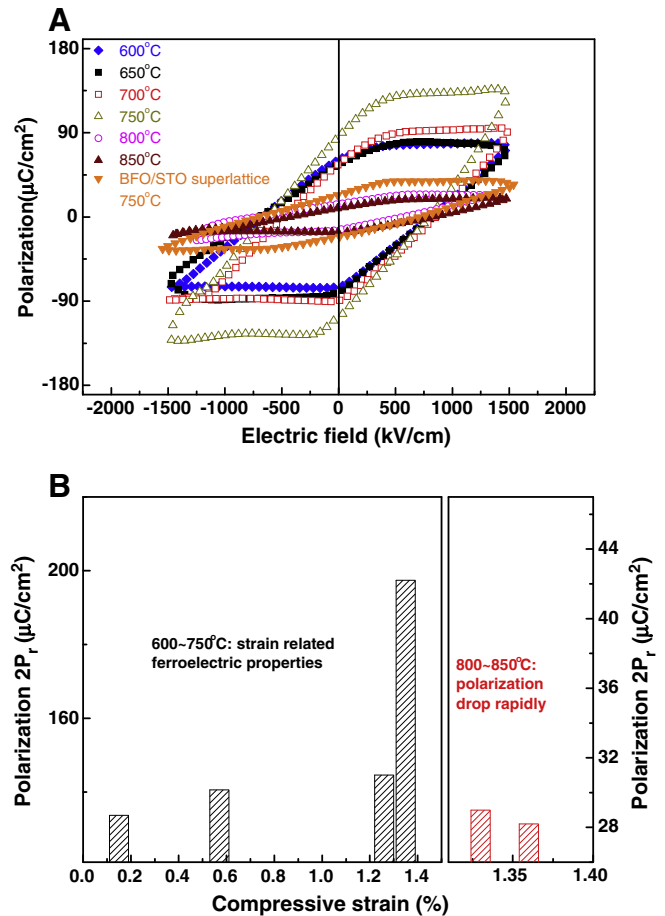

Fig. 5. (A) Electric hysteresis loops of La-doped BFO/STO superlattice films deposited at different substrate temperatures. Hysteresis loops of optimized BFO/STO superlattice films deposited at 750 °C with the same sputtering conditions is also shown in the figure for comparison. (B) The variation of $2P_r$ values with in-plane strain of superlattice structure at different deposition temperatures. Strain enhancement of ferroelectric properties is clearly observed at deposition temperature below 750 °C.

Pendellösung fringes exhibit polarization that increases with deposition temperature. This result is attributable to the in-plane strain, and the attainable polarization ($2P_r$), ranging from 133.7 μC cm^{-2} to 197.4 μC cm^{-2} at deposition temperatures of 600 °C–750 °C, exceeds those of BFO/STO superlattice films that were deposited under similar deposition conditions in our previous study [11]. This finding is strong evidence that La doping enhances the ferroelectric properties of the BFO single layer but also performance of the BFO superlattice structure. Nevertheless, the polarization of superlattice films decreases rapidly at deposition temperature above 800 °C.

Fig. 5(B) plots the variation of $2P_r$ values at different deposition temperatures for a superlattice structure with in-plane strain. La-doped BFO/STO thin superlattice films that were deposited under 750 °C exhibit a positive correlation between polarization values and the in-plane strain; higher in-plane strain leads to greater polarization. However, with their high crystalline quality and distinct superlattice structure, the superlattice films that are deposited at 800 °C and 850 °C have much lower polarization values than the other films, even lower than that of BFO/STO superlattice films in the authors' earlier study [11].

Fig. 6 plots the measured current density as a function of the electric field for a La-doped BFO/STO thin film at room temperature. The figure reveals a typical shape of curve and stable leakage properties of films at a deposition temperature $\leqq$750 °C. Superlattice films at deposition temperature of $\leqq$750 °C also have much lower leakage current densities than did BFO/STO superlattice films in our earlier
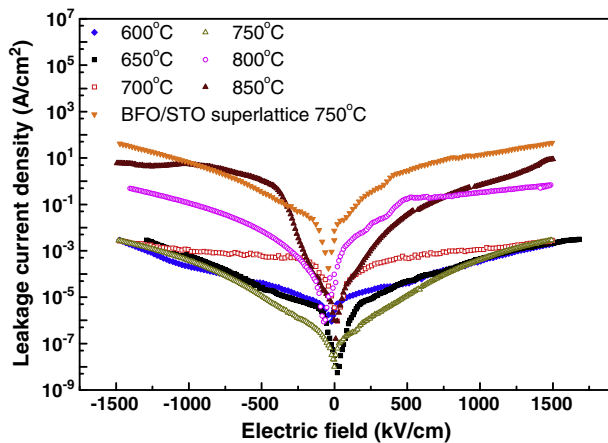
Fig. 6. Leakage current density of La-doped BFO/STO superlattice films versus electric field at different deposition temperatures.

study [11]. A rapidly increasing leakage current density and an asymmetric loop of the leakage current density of the superlattice films are observed at deposition temperatures of over 800 °C, even though the leakage current density remains less than that of BFO/STO films.

In summary, La-doped BFO/STO superlattice films have a stable deposition rate and well leakage and ferroelectric properties that are better than those of BFO/STO superlattice films that are deposited under similar condition [11]. This difference may result from the stronger La–O chemical bond comparing with Bi–O bond to stabilize the structure of BFO [22]. The lower oxygen vacancies and the lower defect like oxygen-deficient dendrite which reduce the leakage and ferroelectric properties of films can generate [26,27]. In this investigation, the strain-induced polarization is observed in La-doped BFO/STO superlattice films. The superlattice films deposited at 700 and 750 °C show enhanced film density, crystalline quality, and polarization. The superlattice films that are deposited at 750 °C are of the highest quality, and have the highest remnant polarization value. As the deposition temperature increases ($\geqq$800 °C), in spite of the high strain state, the polarization value of the superlattice film decreases and the leakage current density increases rapidly. Reducing the film density and increasing the interface/surface roughness imply the increase of defects in superlattice structure, and these factors could degrade the ferroelectric and leakage properties. The results demonstrate that the ferroelectric and leakage properties of the superlattice structure are strongly influenced by crystal quality, strain state and the defect state in the superlattice structure.

4. Conclusions

La-doped BFO/STO superlattice structures with high crystalline quality were fabricated on Nb-doped STO substrate with temperature range of 700–850 °C. Enhanced polarization induced by in-plane strain, originated from epitaxial-growth superlattice structure, is observed. The leakage current of the superlattice is much larger at a temperature above 800 °C, which is consistent with fitting result of film density. La doping has been proved to reduce leakage current and enhance ferroelectric properties in the BFO/STO superlattice films. When growth temperature is higher than 800 °C, the films exhibit lower 2P_r values due to reduced film density, indicating that film density (defect state) is also a key factor, which can influence ferroelectric properties of La-doped BFO/STO superlattice films, in addition to in-plane strain. The lower 2P_r values of superlattice films deposited at temperature higher than 800 °C indicate that the ferroelectric properties of La-doped BFO/STO superlattice structures are enhanced by lattice strain and strongly correlated with the defect state in the superlattice structure.

References

[1] D. Bondurant, F. Gnadinger, IEEE Spectr. 26 (1989) 30.
[2] N.A. Hill, J. Phys. Chem. B 104 (2000) 6694.
[3] X. Qi, J. Dho, R. Tomov, M.G. Blamire, J.L. MacManus-Driscoll, Appl. Phys. Lett. 86 (2005) 062903.
[4] H. Bea, M. Bibes, A. Barthelemy, K. Bouzehouane, E. Jacquet, A. Khodan, J.P. Contour, S. Fusil, F. Wyczisk, A. Forget, D. Lebeugle, D. Colson, M. Viret, Appl. Phys. Lett. 87 (2005) 072508.
[5] T. Shimuta, O. Nakagawara, T. Makino, S. Arui, H. Tabata, T. Kawai, J. Appl. Phys. 91 (2002) 2290.
[6] O. Nakagawara, T. Shimuta, T. Makino, S. Arui, H. Tabata, T. Kawai, Appl. Phys. Lett. 77 (2000) 3257.
[7] J. Kim, L. Kim, D. Jung, Y.S. Kim, I.W. Kim, J.H. Je, J. Lee, Jpn. J. Appl. Phys. 42 (2003) 5901.
[8] R. Ranjith, B. Kundys, W. Prellier, Appl. Phys. Lett. 91 (2007) 222904.
[9] S. Bose, S.B. Krupanidhi, Appl. Phys. Lett. 90 (2007) 212902.
[10] R. Ranjith, R.V.K. Mangalam, Ph. Boullay, A. David, M.B. Lepetit, U. Lüders, W. Prellier, A. Da Costa, A. Ferri, R. Desfeux, Gy. Vincze, Zs. Radi, C. Aruta, Appl. Phys. Lett. 96 (2010) 022902.
[11] S.J. Chiu, Y.T. Liu, H.Y. Lee, G.P. Yu, J.H. Huang, J. Cryst. Growth 334 (2011) 90.
[12] S.T. Zhang, Y. Zhang, M.H. Lu, C.L. Du, Y.F. Chen, Z.G. Liu, Y.Y. Zhu, N.B. Ming, Appl. Phys. Lett. 88 (2006) 162901.
[13] G.L. Yuan, S.W. Or, Appl. Phys. Lett. 88 (2006) 062905.
[14] S.K. Singh, K. Sato, K. Maruyama, H. Ishiwara, Jpn. J. Appl. Phys. 45 (2006) 37.
[15] Y.H. Lee, J.M. Wu, C.H. Lai, Appl. Phys. Lett. 88 (2006) 042903.
[16] B. Yu, M. Li, J. Liu, D. Guo, L. Pei, X. Zhao, J. Phys. D: Appl. Phys. 41 (2008) 065003.
[17] S.K. Singh, H. Ishiwara, Appl. Phys. Lett. 88 (2006) 262908.
[18] C.F. Chung, J.P. Lin, J.M. Wu, Appl. Phys. Lett. 88 (2006) 242909.
[19] J.K. Kim, S.S. Kim, W.J. Kim, A.S. Bhalla, R. Guo, Appl. Phys. Lett. 88 (2006) 132901.
[20] W.M. Zhu, Z.G. Ye, Appl. Phys. Lett. 89 (2006) 232904.
[21] K. Ueda, H. Tabata, T. Kawai, J. Appl. Phys. Lett. 75 (1999) 555.
[22] B.H. Park, B.S. Kang, S.D. Bu, T.W. Noh, J. Lee, W. Joe, Nature 401 (1999) 682.
[23] V.R. Palkar, D.C. Kundaliya, S.K. Malik, J. Appl. Phys. 93 (2003) 4337.
[24] D. Lee, M.G. Kim, S. Ryu, H.M. Jang, S.G. Lee, Appl. Phys. Lett. 86 (2005) 222903.
[25] D.K. Bowen, B.K. Tanner, Nanotechnology 4 (1993) 175.
[26] J.F. Scott, C.A. Araujo, B.M. Melnick, L.D. McMillan, R. Zuleeg, J. Appl. Phys. 70 (1991) 382.
[27] R. Plumlee, Sandia Laboratories Report No. SC-RR-67-730, 1967.